Phys. Status Solidi A **213,** No. 11, 2838–2843 (2016) / **DOI** 10.1002/pssa.201600493

physica status solidi a
www.pss-a.com
applications and materials science

Interactions of hydrogen with vanadium in crystalline silicon

Jack Mullins*, Vladimir P. Markevich, Matthew P. Halsall, and Anthony R. Peaker

Photon Science Institute and School of Electrical and Electronic Engineering, University of Manchester, Manchester M13 9PL, U.K.

Received 13 May 2016, revised 4 July 2016, accepted 5 July 2016
Published online 29 July 2016

Keywords deep-level transient spectroscopy, hydrogen, passivation, silicon, vanadium

* Corresponding author: e-mail jack.mullins@postgrad.manchester.ac.uk, Phone: +44 7857 737 119, Fax: +44 1613 064 770

In this work, we have investigated interactions of vanadium with hydrogen in n- and p-type float zone grown silicon using deep level transient spectroscopy (DLTS), Laplace DLTS, capacitance-voltage and secondary ion mass spectroscopy measurements (SIMS). Vanadium was introduced into Si wafers by ion implantation with subsequent heat treatments at 800 °C for removing the implantation induced lattice damage. In the DLTS spectra of the annealed samples, we have observed two deep level states due to interstitial vanadium (V_i) atoms in n-type Si and one in p-type Si. A comparison of concentration profiles of the V_i atoms with those for the total concentration of V measured by SIMS has shown that at the projected implantation depth the $[V_i]/[V_{total}]$ ratio is less than 0.05 at chemical concentration of vanadium of 1×10^{15} cm^{-3}, so the majority of *V* atoms are in electrically inactive states in this region. At lower chemical concentrations of vanadium, similar values of $[V_i]$ and $[V_{total}]$ are observed. After the treatment of the n-type V-doped samples in a remote hydrogen plasma at room temperature, we have found that the concentration of the V_i atoms decreases while additional electron traps emerge in the DLTS spectra. A trap with the highest concentration has been attributed to a vanadium–hydrogen complex. In the p-type Si:V samples, no new levels have emerged in the DLTS spectra after the H-plasma treatments. It is suggested that in p-type Si:V an interaction of H atoms with the V_i atoms is suppressed because of the Coulombic repulsion of positively charged V_i and hydrogen defects. It is argued that no electrically active defects are formed in either the n- or p-type Si:V samples due to possible interactions of hydrogen with electrically inactive V-related defects. We present evidence that annealing of the n-type Si:V samples in the temperature range 75–125 °C following the application of hydrogen plasma results in up to 20% decrease in the total concentration of electrically active V-related defects, indicating the formation of some electrically inactive V–H complexes. Heat treatments at temperatures above 175 °C have resulted in the disappearance of all the V–H complexes and recovery of electrical activity of the V_i atoms.

1 Introduction In the last decade, the solar photovoltaic industry has grown dramatically and cell costs fallen sharply [1]. This has resulted in a move away from high purity electronic grade silicon. Typically, this is produced by Czochralski or float zone growth from polycrystalline feedstock manufactured by the Siemens process. This route requires a significant amount of high temperature processing and so, such feedstock material is too expensive for the manufacture of crystalline silicon used in photovoltaics [2].

In its place there has been a rise in the manufacture of upgraded metallurgical grade silicon (UMG-Si) and block cast multicrystalline silicon (mc-Si), the latter of which has held over 60% of the PV market since 2011 [3]. A comprehensive review of solar silicon material technologies and their market position appears in Ref. [4]. UMG-Si and mc-Si provide a lower cost per kWh in finished cells than those made using single crystal silicon. However, the best mc-Si cell and module efficiencies are ∼5% lower than the best manufactured from single crystal silicon [5] and although figures for UMG-Si are much more variable, a typical best figure is ∼10% lower than single crystal cells.

The reduced efficiency of mc- and UMG-Si cells is primarily due to the higher concentration of impurities originating from the UMG-Si feedstock or from the crucible used for mc-Si growth. These impurities reduce the carrier lifetime via the introduction Shockley–Read–Hall recombination centres as electrically active deep-level states in the band gap [6]. Of particular concern are transition metal

impurities, which have been shown to have an important effect on minority carrier lifetime and cell efficiency even at low concentrations [3, 7, 8]. Although the concentration of transition metal impurities is extremely low in single crystal material ($<10^{10}\,cm^{-3}$), it can be orders of magnitude higher in upgraded metallurgical (UMG) and mc-Si [9, 10]. Reducing the concentration or the detrimental effect of these impurities on minority carrier lifetime would allow the fabrication of more efficient low-cost cells.

It is well known that the introduction of hydrogen (e.g. through the application of silicon nitride anti-reflective films) reduces surface recombination. Recently, it has been shown that hydrogen can also passivate electrically active defects in the bulk of the silicon, increasing minority carrier lifetime [11, 12]. However, the mechanism by which passivation occurs is not well-understood and is the subject of some controversy.

Vanadium is a transition metal impurity present in UMG Silicon and mc-Si grown from feedstock that has not been purified by the Siemens process. Previous work has shown that it has a large impact on solar cell efficiency at concentrations as low as $10^{12}\,cm^{-3}$ [7]. Further, the low diffusivity of vanadium in silicon makes it particularly difficult to getter.

In this work, we investigate the interactions between hydrogen and vanadium in silicon, in order to determine whether electrically active vanadium can be effectively passivated.

2 Experimental We have studied the electrical activity of vanadium in silicon using deep level transient spectroscopy (DLTS), Laplace DLTS and capacitance–voltage (*C–V*) measurements. We have also used secondary ion mass spectrometry (SIMS) in order to determine the total metallurgical vanadium content and the relative abundance of electrically active interstitial vanadium (V_i).

In this work, wafers of n- and p-type float zone silicon with resistivity in the range 1–5 Ω cm were used. Vanadium was introduced into these wafers by ion implantation at energies of 2 MeV (n-type) and 1.3 MeV (p-type) with doses of $2.5\times10^{11}\,cm^{-2}$ and $2.6\times10^{11}\,cm^{-2}$, respectively. These implantations were expected to result in peak concentrations of $4.8\times10^{15}\,cm^{-3}$ in n-type and 5.7×10^{15} in p-type Si.

Strips of silicon were cut from the centre of the implanted wafers. These strips were RCA cleaned and annealed for 30 min in the temperature range 700–900 °C in nitrogen in order to remove implantation damage. Hydrogen was introduced into the strips through exposure to a 50 W remote H plasma at room temperature for 30 min before they were prepared for electrical measurements (DLTS, Laplace DLTS, capacitance–voltage and current–voltage (*I–V*) measurements). Schottky barrier diodes (SBDs) were formed on the implanted surface of these samples by thermal evaporation of Au through a shadow mask on n-type samples, and through plasma sputtering of Ti and Al on the p-type samples. An Ohmic contact was deposited on the back surface using thermal evaporation of Al on n-type and Au on p-type samples. The quality of the diodes was tested using *C–V* and *I–V* measurements. These measurements provided the concentration of shallow uncompensated donors or acceptors and the probing depth achievable in capacitance measurements.

DLTS and Laplace DLTS measurements were carried out on both n- and p-type Si samples in order to characterise deep level electronic defects. N-type Si samples were also studied using 30-min isochronal annealing in the temperature range 75–200 °C and isothermal annealing at 100 °C with durations between 30 and 200 min. Following each anneal, *C–V* and *I–V* measurements were carried out and DLTS and Laplace DLTS were undertaken.

3 Results and discussion

3.1 Electrically active defects in vanadium-implanted and annealed Si Figure 1 shows conventional DLTS spectra recorded on vanadium implanted n- and p-type float zone Si samples, which were annealed at 800 °C for 30 min.

In the spectrum for the n-type Si sample (spectrum 2) two clear signals are visible as peaks with their maxima at 115 and 205 K, denoted in Fig. 1 as E_1 and E_2. The activation energies for electron emission from the levels associated with these peaks were determined from Arrhenius plots of T^2 corrected electron emission rates measured using Laplace DLTS as 0.20 eV (E_1) and 0.43 eV (E_2) from the conduction band. Nearly equal magnitudes of the E_1 and E_2 traps indicate that the concentrations of the corresponding traps are equal. We will show in the following sections that the absolute concentrations, concentration profiles and annealing behaviour of the E_1 and E_2 traps are nearly identical. These facts provide a strong basis for the assignment of the traps to two energy levels of the same defect. The values of the electron emission energies for the E_1 and E_2 traps are

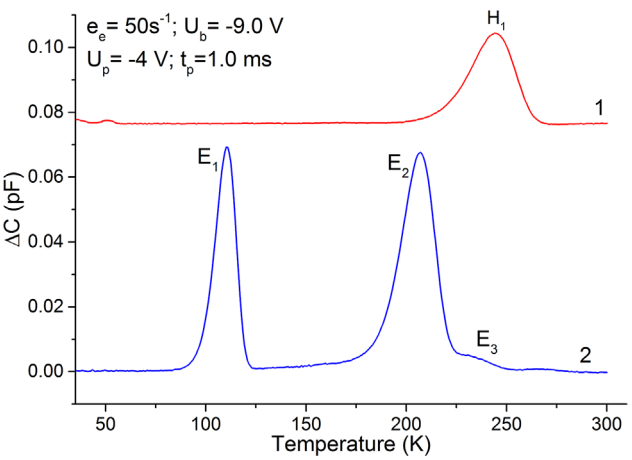

Figure 1 DLTS spectra of vanadium implanted p-type (spectrum 1) and n-type (spectrum 2) float zone silicon samples, which were annealed at 800 °C for 30 min. Measurement settings are shown on the graph. Spectrum 1 is shifted on the vertical axis for clarity.

close to those measured for interstitial vanadium in previous studies [13, 14] in which the V_i defect was found to have an acceptor level and a donor level at 0.20 and 0.45 eV below the conduction band edge, respectively. There is also a minor DLTS signal denoted as E_3 in spectrum 2 (Fig. 1). The parameters and origin of the trap, which gives rise to this signal, will be discussed in more details below.

In the spectrum for p-type silicon (spectrum 1 in Fig. 1), one DLTS signal with its peak maximum at 240 K is observed. It is denoted as H_1 in Fig. 1. We have measured the activation energy for hole emission from the corresponding trap as 0.46 eV from the valence band. The hole capture cross section for this trap is found to be temperature dependent and an energy barrier for capture has been determined as 0.12 eV. The above values are very close to those determined previously for the dominant hole trap in vanadium doped p-type silicon crystals [14, 15]. This trap was attributed to the second donor level of interstitial vanadium [14, 15].

The DLTS spectra shown in Fig. 1 resemble those presented in the literature for V-doped silicon [13–15]. A comparison of the parameters of the dominant traps with those determined previously for interstitial vanadium in Si [13–16] allows us to assign the E_1 and E_2 traps to the acceptor and first donor levels of the V_i defect, and the H_1 trap to the second donor level of this centre.

3.2 Comparison of vanadium concentration profiles measured by SIMS and DLTS Figure 2 shows the results of SIMS measurements carried out on vanadium implanted n- and p-type float zone silicon samples after implantation and annealing at 800 °C. These measurements provide the total chemical concentration of vanadium in the samples which are then compared to the concentration of electrically active defects measured via DLTS.

The SIMS data presented in Fig. 2 show that the implanted vanadium is present at a peak concentration of 10^{15} cm^{-3} in the samples annealed at 800 °C. However, DLTS measurements of the electrically active interstitial fraction in these samples have provided concentrations of the order of 10^{13} cm^{-3}. From this we can determine that only a small fraction of vanadium in silicon (around 2%) is electrically active when the chemical concentration is 10^{15} cm^{-3}. It is not possible from this work to determine accurately the $[V_i]/[V_{total}]$ ratio at lower chemical concentrations because of the SIMS detectivity but it is certainly considerably higher than that at the implant peak. Figure 2 also shows that the concentration of the E_1 and E_2 traps nearly coincide in the annealed n-type samples, confirming that these are related to two energy levels of the interstitial vanadium defect. The large difference between the chemical concentration and concentration of the electrically active V_i defect in the annealed samples in the regions close to the projected depth suggests that the remaining vanadium either occupies substitutional sites or some precipitation occurs in these regions.

A comparison of the SIMS profiles following annealing at 800 °C with those for the as-implanted samples shows that the vanadium peak concentration decreases upon annealing. This is most likely due to diffusion of the vanadium to the surface and bulk of the samples.

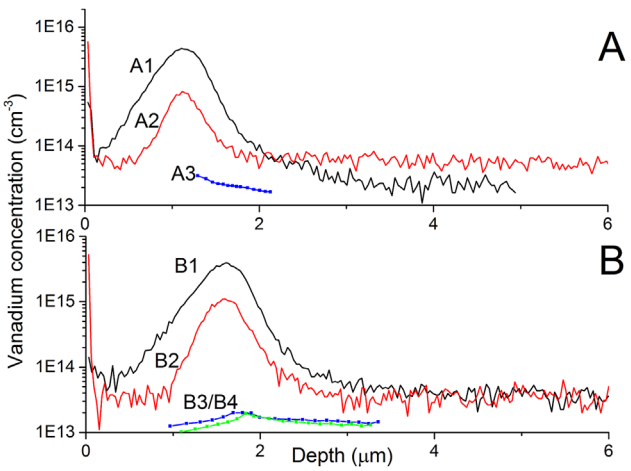

Figure 2 LDLTS measurements of the concentration of electrically active vanadium compared to SIMS measurements of the total (chemical) concentration of vanadium in vanadium implanted p-type (plot A) and n-type (plot B) float zone silicon. SIMS measurements were carried out on as implanted samples (curves A1 and B1), and samples annealed at 800 °C (curves A2 and B2). LDLTS measurements were carried out on the 800 °C annealed sample only and are shown for the level H_1 in p-type (curve A3) and for the levels E_1 and E_2 in n-type (curves B3/B4).

3.3 Interactions of vanadium with hydrogen Figure 3 shows conventional DLTS spectra of vanadium implanted n- and p-type float zone Si following annealing at

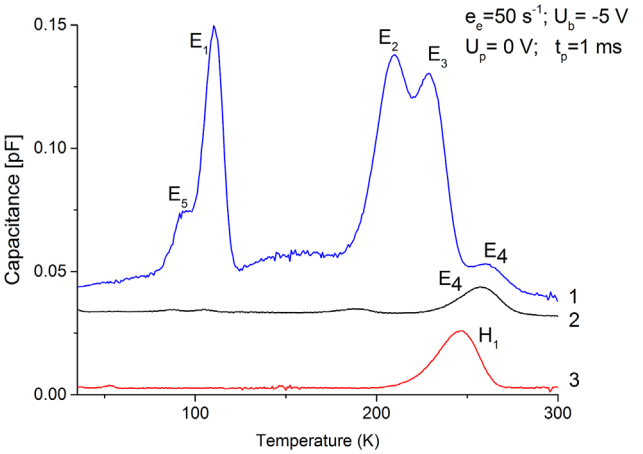

Figure 3 DLTS spectra following annealing at 800 °C and application of a 50 W remote plasma for 30 min at room temperature to as grown n-type (curve 2), vanadium implanted p-type (curve 3) and n-type (curve 1) float zone silicon. Measurement settings are shown on the graph. The spectra are shifted on the vertical axis for clarity.

800 °C and the application of a 50 W remote hydrogen plasma for 30 min at room temperature.

The only signal observed in the conventional DLTS spectrum of p-type silicon after the remote plasma treatment (spectrum 3 in Fig. 3) is identical to the H_1 signal due to the second donor level of V_i seen in the spectrum of the sample which was not treated in the plasma (spectrum 1 in Fig. 1). The concentration of interstitial vanadium in the hydrogenated p-type silicon has been determined using Laplace DLTS and *C*–*V* measurements. It does not differ significantly from that measured before the application of hydrogen plasma.

In the DLTS spectrum of the hydrogenated n-type sample (spectrum 1 in Fig. 3), in addition to the E_1 and E_2 signals due to V_i shown in Fig. 1 we have observed three new signals, denoted as E_3, E_4 and E_5 in Fig. 3. The E_4 signal has also been observed in a control non-implanted sample which had undergone the same processing steps and H-plasma treatment. As such the defect, which gives rise to the E_4 signal is likely a result of the H-plasma treatment, and not related to vanadium.

The properties of the E_3 trap have been determined using *C*–*V* measurements and LDLTS. We find that the state is donor like and the activation energy for electron emission is 0.51 eV from the conduction band. This value is close to that observed in a previous study [13] of vanadium in silicon, in which a similar signal was seen in a DLTS spectrum for a sample with in-diffused vanadium, which was etched in a solution containing HF. The authors of Ref. [13] assigned this signal to a vanadium–hydrogen complex, and determined the activation energy for electron emission from the corresponding level as 0.50 eV from the conduction band.

The results of concentration profile measurements of the vanadium related defects in the hydrogenated n-type silicon sample are presented in Fig. 4. The concentration profiles of the interstitial vanadium (E_1 and E_2 traps) and the vanadium–hydrogen complex (E_3) plotted in Fig. 4 show that the vanadium–hydrogen complex forms in greater concentration close to the surface, as expected due to the increased hydrogen concentration in the near surface region. The concentrations of the two interstitial vanadium related levels decrease sharply towards the surface. It is likely that this decrease is associated with the interaction of interstitial vanadium atoms with the in-diffused hydrogen atoms. Finally, the shoulder seen in Fig. 3 at 95 K (E_5) is found to have a much lower concentration than the other traps, although its concentration rises slightly towards the surface. From our measurements, the origin of this shoulder is unclear; however, it can be suggested that it is related to another vanadium–hydrogen complex.

An analysis of the data presented in Figs. 2 and 4 show that the concentrations of the hydrogenation-induced electrically active traps do not exceed the concentration of interstitial vanadium at any depth and are much lower than the concentration of electrically inert vanadium defects at the projected implantation depth. So, it is unlikely that a possible interaction of introduced hydrogen atoms with the electrically inert vanadium defects causes the formation of some electrically active complexes.

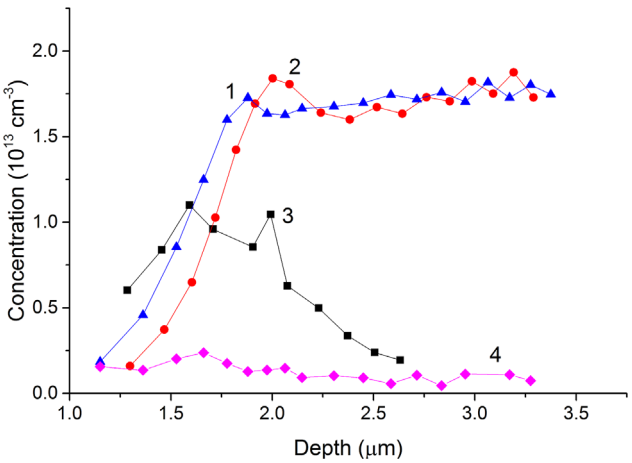

Figure 4 Concentration–depth plots of vanadium related defects in float zone grown n-Si implanted with vanadium following annealing at 800 °C for 30 min and application of a 50 W remote hydrogen plasma for 30 min at room temperature. Curves 1, 2 and 3 represent defects labelled E_1, E_2 and E_3 in Fig. 3, while curve 4 represents E_5.

In order to establish whether the concentration of the vanadium–hydrogen complex could be increased, or whether other vanadium hydrogen complexes (including electrically inactive ones) could be formed, isothermal and isochronal anneals were carried out on the hydrogenated n-type silicon samples.

3.4 Effect of annealing Changes in the DLTS spectra of n-type silicon samples following a series of 30 min isochronal anneals in the temperature range 75–200 °C are shown in Fig. 5. The spectra presented in Fig. 5 show that annealing changes the spectra significantly for temperatures higher than 150 °C. We find that annealing at 75 °C increases the V–H concentration while the V_i concentration remains unchanged. Annealing at temperatures between 100 and 125 °C reduces the measured concentration of all electrically active defects, while annealing at 150 °C increases the V_i concentration while the V–H concentration remains unchanged.

Annealing at 175 and 200 °C is seen to result in completely dissociation of the V–H complex (E_3 trap) and an increase in the interstitial vanadium concentration to the levels similar to those measured in samples which had not undergone plasma treatment. This result is consistent with the behaviour of the V–H complex observed in Ref. [13], in which the concentration of a V–H complex was found to be below detection limits following annealing at 175 °C.

The concentrations of each of the electrically active defects measured following annealing at 125 °C and after the dissociation of hydrogen related defects at 200 °C are shown in Fig. 6 for clarity. A reduction in the total concentration of electrically active defects of around 20%

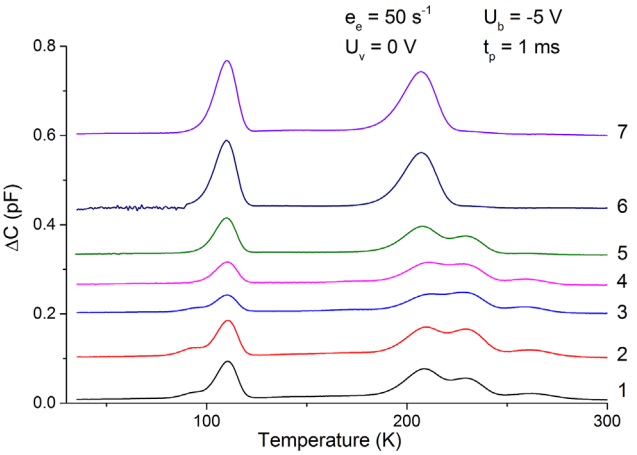

Figure 5 DLTS spectra of vanadium implanted n-type float zone silicon, following annealing at 800 °C and application of a 50 W remote plasma for 30 min (curve 1) as well as sequential anneals at temperatures 75 °C (curve 2), 100 °C (curve 3), 125 °C (curve 4), 150 °C (curve 5), 175 °C (curve 6) and 200 °C (curve 7) for 30 min. Measurement settings are shown on the graph. The spectra are shifted on the vertical axis for clarity.

has occurred following the application of hydrogen plasma and a 30 min anneal at 125 °C.

The observation of a reduction in the total concentration of electrically active vanadium-related defects upon annealing at 100 and 125 °C suggests that some electrically inert defects containing vanadium atoms are forming at these temperatures.

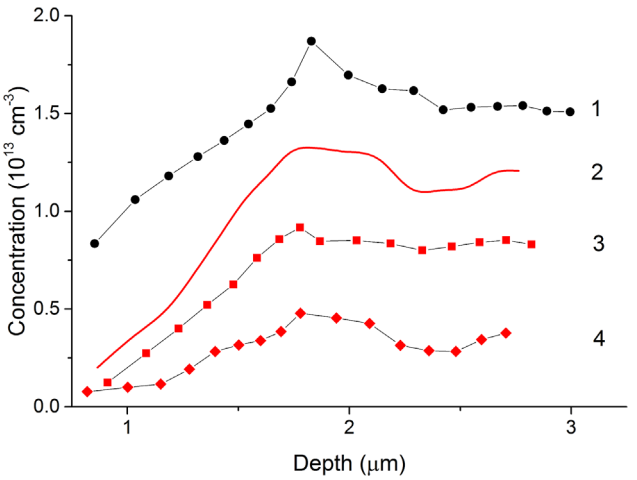

Figure 6 Defect concentration in float zone grown n-Si with resistivity 2.5 Ω cm implanted with vanadium following annealing at 800 °C and application of a 50 W remote hydrogen plasma for 30 min at room temperature as well as annealing at 125 °C (curves 2, 3 and 4) and at 200 °C (curve 1) for 30 min. Curves 3 and 4 show measured V_i and V–H concentration after annealing at 125 °C, while curve 2 shows the calculated sum of the two. After 200 °C annealing only V_i is observed and its concentration is shown in curve 1.

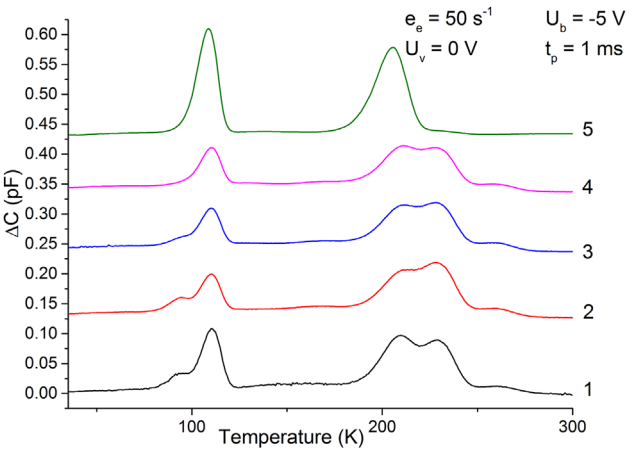

Figure 7 DLTS spectra of vanadium implanted n-type float zone silicon with resistivity 2.5 Ω cm, following annealing at 800 °C and application of a 50 W remote plasma for 30 min (curve 1) as well as sequential anneals at 100 °C of duration 30 min (curve 2), 60 min (curve 3) and 200 min (curve 4). These are compared to DLTS spectra taken following a 200 °C–30 min anneal shown by curve 5. Measurement settings are shown on the graph. The spectra are shifted on the vertical axis for clarity.

In an attempt to reduce the concentration of electrically active vanadium as much as possible, we studied the changes in concentration of electrically active defects following a series of isothermal anneals at 100 °C, with duration between 30 and 200 min using DLTS and *C–V* measurements.

DLTS spectra measured after sequential isothermal anneals are displayed in Fig. 7. We observe a reduction in the concentration of all of the vanadium-related defects following each anneal. We see that the total concentration drops rapidly in the first 60 min of cumulative annealing. Subsequent anneals have a significantly smaller effect on the concentration, and their effect is negligible after 200 min.

Annealing for 30 min at 200 °C has resulted in the dissociation of the vanadium–hydrogen complex and recovery of electrically active interstitial vanadium.

The results displayed in Figs. 5–7 show that a fraction of electrically active vanadium can be passivated in n-type silicon following the introduction of hydrogen and appropriate thermal treatment. However, the reduction of the electrically active defect concentration is significantly lower than that observed in previous studies for similar transition metals, (e.g. titanium [17]) in which total passivation of electrically active defects was observed.

4 Conclusions In this study, a comparison of SIMS and DLTS measurements has shown that under the implantation and annealing (800 °C) conditions we used only a small portion of vanadium in silicon is electrically active (about 2% of the chemical concentration) at the highest chemical concentration studied (1×10^{15} cm^{-3}). The analysis of the SIMS and DLTS data shows that beyond the regions with high chemical concentration of vanadium,

[V_{total}], the concentration of electrically active interstitial vanadium is about $2 \times 10^{13}\,cm^{-3}$ and is close to the chemical concentration. We have observed two levels due to interstitial vanadium in n-type silicon with activation energies 0.20 and 0.45 eV from the conduction band and one in p-type silicon with activation energy 0.46 eV from the valence band, in agreement with previous works.

In n-type silicon, the introduction of hydrogen leads to the formation of a vanadium–hydrogen complex at room temperature due to an interaction of mobile H atoms with interstitial vanadium atoms. Annealing of hydrogenated samples at temperatures between 100 and 150 °C has resulted in a decrease of the concentrations of electrically active V_i and V–H complexes, suggesting that some electrically inert species could be formed. The maximum reduction of the total concentration of electrically active defects was found to be around 20%. In p-type silicon, the Coulombic repulsion of positively charged hydrogen and vanadium ions prevents the formation of V–H complexes.

Acknowledgements This work has been supported by the ESPRC under the Supergen contract EP/M024911/1. The SIMS measurements were undertaken by Dr. Alison Chew of Loughborough Surface Analysis Ltd.

References

[1] G. Coletti, I. Gordon, M. C. Shubert, W. Warta, E. J. Ovrelid, A. Jouini, M. Tucci, and G. de Cesare, Sol. Energy Mater. Sol. Cells **130**, 629 (2014).
[2] S. Pizzini, Sol. Energy Mater. Sol. Cells **94**, 1528 (2010).
[3] Y. M. Yang, A. Yu, B. Hsu, W. C. Hsu, A. Yang, and C. W. Lan, Prog. Photovolt.: Res. Appl. **23**, 340 (2015).
[4] G. Bye and B. Ceccaroli, Sol. Energy Mater. Sol. Cells **130**, 634 (2014).
[5] M. A. Green, K. Emery, Y. Hishikawa, W. Warta, and E. D. Dunlop, Prog. Photovolt.: Res. Appl. **23**, 805 (2015).
[6] A. R. Peaker, V. P. Markevich, B. Hamilton, G. Parada, A. Dudas, A. Pap, E. Don, B. Lim, J. Schmidt, L. Yu, Y. Yoon, and G. Rozgonyi, Phys. Status Solidi A **209**, 1884 (2012).
[7] J. R. Davis, A. Rohatgi, R. H. Hopkins, P. D. Blais, P. Rai-Choudhury, J. R. McCormick, and H. C. Mollenkopf, IEEE Trans. Electron Devices **27**, 677 (1980).
[8] G. Coletti, P. C. P. Bronsveld, G. Hahn, W. Warta, D. Macdonald, B. Ceccaroli, K. Wambach, Nam Le Quang, and J. M. Fernandez, Adv. Funct. Mater. **21**, 890 (2011).
[9] A. A. Istratov, T. Buonassisi, R. J. McDonald, A. R. Smith, R. Schindler, J. A. Rand, J. P. Kalejs, and E. R. Weber, J. Appl. Phys. **209**, 6552 (2003).
[10] J. Hampel, F. M. Boldt, H. Gerstenberg, G. Hampel, J. V. Kratz, S. Reber, and N. Wiehl, Appl. Radiat. Isotopes **69**, 1365 (2011).
[11] B. J. Hallam, P. G. Hamer, S. R. Wenham, M. D. Abbott, A. Sugianto, A. M. Wenham, C. E. Chan, X. GuangQi, J. Kraiem, J. Degoulange, and R. Einhaus, IEEE J. Photovoltaics **4**, 88 (2014).
[12] AnYao Liu, Chang Sun, and D. Macdonald, J. Appl. Phys. **116**, 194902 (2014).
[13] T. Sadoh, H. Nakashima, and T. Tsurushima, J. Appl. Phys. **72**, 520 (1992).
[14] L. Tilly, H. G. Grimmeiss, H. Pettersson, K. Schmalz, K. Tittelbach, and H. Kerkow, Phys. Rev. B **44**, 809 (1991).
[15] R. Pässler, H. Petterson, H. G. Grimmeiss, and K. Schmalz, Phys. Rev. B **55**, 4312 (1997).
[16] A. G. Marinopoulos, P. Santos, and J. Coutinho, Phys. Rev. B **92**, 075124 (2015).
[17] S. Leonard, V. P. Markevich, A. R. Peaker, and B. Hamilton, Appl. Phys. Lett. **103**, 132103 (2013).